JACS
JOURNAL OF THE AMERICAN CHEMICAL SOCIETY
pubs.acs.org/JACS
Communication

Ladder Phenylenes Synthesized on Au(111) Surface via Selective [2+2] Cycloaddition

Deng-Yuan Li,[#] Xia Qiu,[#] Shi-Wen Li,[#] Yin-Ti Ren,[#] Ya-Cheng Zhu, Chen-Hui Shu, Xiao-Yu Hou, Mengxi Liu,* Xing-Qiang Shi,* Xiaohui Qiu,* and Pei-Nian Liu*

Cite This: J. Am. Chem. Soc. 2021, 143, 12955−12960
Read Online
ACCESS | Metrics & More | Article Recommendations | Supporting Information

ABSTRACT: Ladder phenylenes (LPs) composed of alternating fused benzene and cyclobutadiene rings have been synthesized in solution with a maximum length no longer than five units. Longer polymeric LPs have not been obtained so far because of their poor stability and insolubility. Here, we report the synthesis of linear LP chains on the Au(111) surface via dehalogenative [2+2] cycloaddition, in which the steric hindrance of the methyl groups in the 1,2,4,5-tetrabromo-3,6-dimethylbenzene precursor improves the chemoselectivity as well as the orientation orderliness. By combining scanning tunneling microscopy and noncontact atomic force microscopy, we determined the atomic structure and the electronic properties of the LP chains on the metallic substrate and NaCl/Au(111). The tunneling spectroscopy measurements revealed the charged state of chains on the NaCl layer, and this finding is supported by density functional theory calculations, which predict an indirect bandgap and antiferromagnetism in the polymeric LP chains.

Conjugated ladder polymers have attracted intense attention because of their intriguing properties, which are distinct from those of conventional conjugated polymers.[1−7] As a result of their fully conjugated and rigid polymer backbones, conjugated ladder polymers possess some intriguing properties,[2−12] including high charge carrier mobilities,[8,9] long exciton diffusion lengths,[10] and low energy gaps.[2,11,12] Ladder phenylenes (LPs) represent a unique family of conjugated ladder polymers, comprising one-dimensional ladder chains of linearly alternating fused benzene and cyclobutadiene rings.[13,14] Because of the unusual combination of aromatic and antiaromatic moieties, LPs are expected to possess unique optical and electronic properties and are considered promising materials for applications in optoelectronic devices.[15−21] Ever since the pioneering synthesis of biphenylene by Hosaeus,[22] many efforts have been made to synthesize LP chains.[13,14,23−25] To date, the longest prepared LPs have contained five benzene units,[17,25] and the synthesis of longer, polymeric LPs remains a great challenge. Moreover, experimental investigation of the properties of existing LPs has been limited to collecting the average signals of ensembles of LP molecules.[23,26−29] Thus, the synthesis and characterization of individual LPs have not been achieved, which severely hampered the exploration of the properties of these unusual conjugated ladder polymers.

On-surface synthesis provides a versatile and convenient route for the atomically precise fabrication of insoluble benzenoid macromolecules,[30,31] ranging from single molecules,[32−37] one-dimensional polymers,[38−42] and graphene nanoribbons[43−48] to two-dimensional covalent networks[49−53] because of the solvent-free and ultra-high-vacuum conditions. Another advantage is that the submolecular structures and electronic properties of the product can be readily achieved by using scanning probe techniques.[54] The most straightforward way to synthesize LPs on surfaces is through the dehalogenative [2+2] cycloaddition of *ortho*-dihalogenated arenes. In the pioneering work of Fasel and Meunier et al., the cycloaddition reactions of *ortho*-dihalotetracenes on an Ag(111) substrate gave multiple products, including tetracene dimers, trimers, and tetramers.[55] Recently, Lin and Kim independently elucidated the mechanism of the metal-mediated dehalogenative [2+2] cycloaddition and concurrent [2+2+2] cycloaddition with 2,3,6,7,10,11-hexabromotriphenylene as the precursor.[56,57] Overall, improving the selectivity of dehalogenative [2+2] cycloaddition is crucial to realizing the on-surface synthesis and characterization of LPs (Figure 1a).

For surface-confined reactions, steric hindrance plays an important role in modulating the reaction pathways and even determining the final products.[58−62] By exploiting steric hindrance, herein we report the synthesis of LPs on a Au(111) surface via highly selective [2+2] cycloaddition; specifically, the noncovalent interactions of the methyl groups of the 1,2,4,5-tetrabromo-3,6-dimethylbenzene (TBDMB) precursor improve the chemoselectivity and the orientational order of the product (Figure 1b), whose atomic structure and electronic states of the LPs are determined by scanning tunneling microscopy/spectroscopy (STM/STS) and noncontact atomic force microscopy (nc-AFM).

LPs with methyl-modified edges were fabricated by the surface-assisted debrominative [2+2] cycloaddition of

Received: May 31, 2021
Published: August 16, 2021

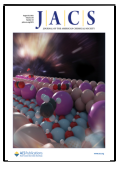

https://doi.org/10.1021/jacs.1c05586
J. Am. Chem. Soc. 2021, 143, 12955−12960

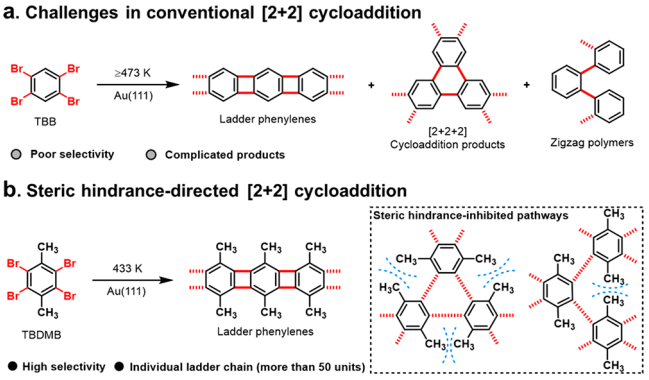

Figure 1. Strategy for the synthesis of LPs. (a) Challenges in conventional [2+2] cycloaddition. (b) Steric hindrance-directed [2+2] cycloaddition.

TBDMB, as shown in Figure 1b. The TBDMB molecules were sublimed onto the Au(111) surface held at 250 K under ultra-high-vacuum conditions. The sample was then cooled to 120 K for further characterization. The STM image (Figure S1 in the Supporting Information) shows a close-packed monolayer structure in which most of the molecules are intact, having a hexagonal structure owing to the repulsion of the bromine substituents (indicated by the white-dotted circle in Figure S1b). The corners in the hexagonal structure could be assigned to four C−Br moieties and two methyl groups of TBDMB (Figure S1b). After annealing at 433 K, most of the TBDMB molecules were desorbed from the Au(111) surface and only a few short chains were absorbed along the edges of the terrace on the Au(111) surface; these could be assigned to linear Me-substituted ladder phenylenes derived from the [2+2] cycloaddition of TBDMB (Figure S1c).

Next, we attempted to dose TBDMB on the Au(111) surface held at 433 K in the hope of obtaining more and longer Me-substituted LPs. The large-scale STM images (Figure 2a) show many linear chain structures distributed on the Au(111) surface, most of which are individual and tend to align with $[11\bar{2}]$ or the equivalent orientations of the Au(111) substrate. The length distribution of the chains follows a log-normal distribution peaking at approximately 5 nm, with some chains extending to approximately 20 nm (more than 50 units) (Figure 2b, inset). The statistical analysis by counting the number of non-cyclobutadiene versus cyclobutadiene reveals that the chemoselectivity of [2+2] cycloaddition is greater than 95%. The high-resolution STM image (Figure 2b) reveals that the individual chain is surrounded by close-packed spherical structures (indicated by white-dotted circles in Figure 2b), which are most likely bromine atoms derived from the debromination of TBDMB molecules. The STM image of a single chain obtained at the indicated tunneling bias shows periodic features with a pitch of 0.38 ± 0.02 nm between adjacent protrusions (Figure 2c). This observation is consistent with our simulated STM image of an LP chain (Figure 2e), which shows a similar periodicity of 0.38 nm, corresponding to the Me-substituted phenylene and cyclobutadiene units. A careful comparison of the experimental and calculated results suggests that the bright protrusions from the backbone of the chain can be assigned to cyclobutadiene groups (indicated by the red dotted circle in Figure 2c), and the dark protrusions at the edge of the chain can be assigned to the methyl groups (indicated by the blue-dotted circles in Figure 2c).

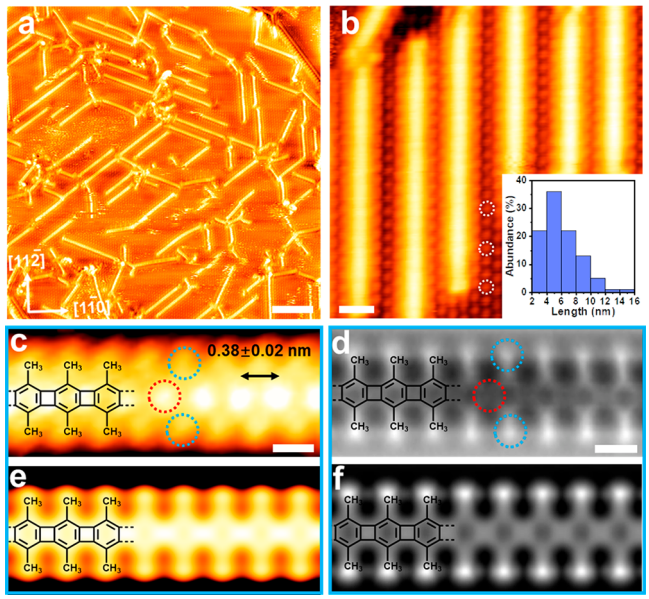

Figure 2. Synthesis and structural characterization of LPs on the Au(111) surface. (a) Overview STM image of LPs after dosing TBDMB on Au(111) held at 433 K. (b) Zoomed-in STM image of LPs surrounded by bromine atoms. The inset is a length distribution of the LPs on the Au(111) surface. (c) STM image of a segment of a single LP chain at the indicated tunneling parameters and (e) the corresponding simulation. (d) nc-AFM image of a segment of a single LP chain and (f) the corresponding simulation. White, blue, and red dotted circles in (b) and (d) indicate bromine atoms and methyl and cyclobutadiene groups of LPs, respectively. Scale bars: (a) 10 nm, (b) 2 nm, (c, d) 0.5 nm. Tunneling parameters: (a) $U = -1.63$ V, $I = 0.55$ nA; (b) $U = -1.20$ V, $I = 0.33$ nA; (c) $U = 1.50$ V, $I = 0.47$ nA; (d) $\Delta z = 30$ pm at set point: $U = -0.5$ V, $I = 0.2$ nA.

To identify the chemical structure of the as-synthesized chains, nc-AFM measurements were performed. The high-resolution nc-AFM image (Figure 2d) reveals that hexagons and tetragons are alternately arranged along the axis of the chain, whereas two protruding arrays are attached to the opposite edge of the chain. Considering the steric configuration, the arrayed protrusions can be assigned to the methyl groups (indicated by the blue-dotted circles in Figure 2d), which is supported by the consistency between the experimental nc-AFM image and the corresponding density functional theory (DFT) simulation (Figure 2f). Moreover, the high-resolution STM (Figure S2a) and nc-AFM images of the chain end (Figure S2b) show a similar contrast to that of the conjugated backbone structure, which can be attributed to the passivation of the ends by hydrogen atoms.[63]

After further annealing to 473 K, most of the chains remained intact (Figure S3b), whereas annealing to 513 K led to the formation of kinks at the chain ends (Figure S3c). These joints are most likely nonplanar structures composed of carbon pentagons and hexagons (Figure S4), which can be attributed to the C−H activation of the methyl groups induced by the high temperature.

To demonstrate the effect of the steric hindrance of the substituents in improving the selectivity of the [2+2] cycloaddition reaction, we performed a control experiment using 1,2,4,5-tetrabromobenzene (TBB), which does not contain methyl groups, as a precursor (Figure S5). The large-scale STM images obtained after dosing Au(111) with TBB by holding the sample at the evaluated temperatures show

https://doi.org/10.1021/jacs.1c05586
J. Am. Chem. Soc. 2021, 143, 12955−12960

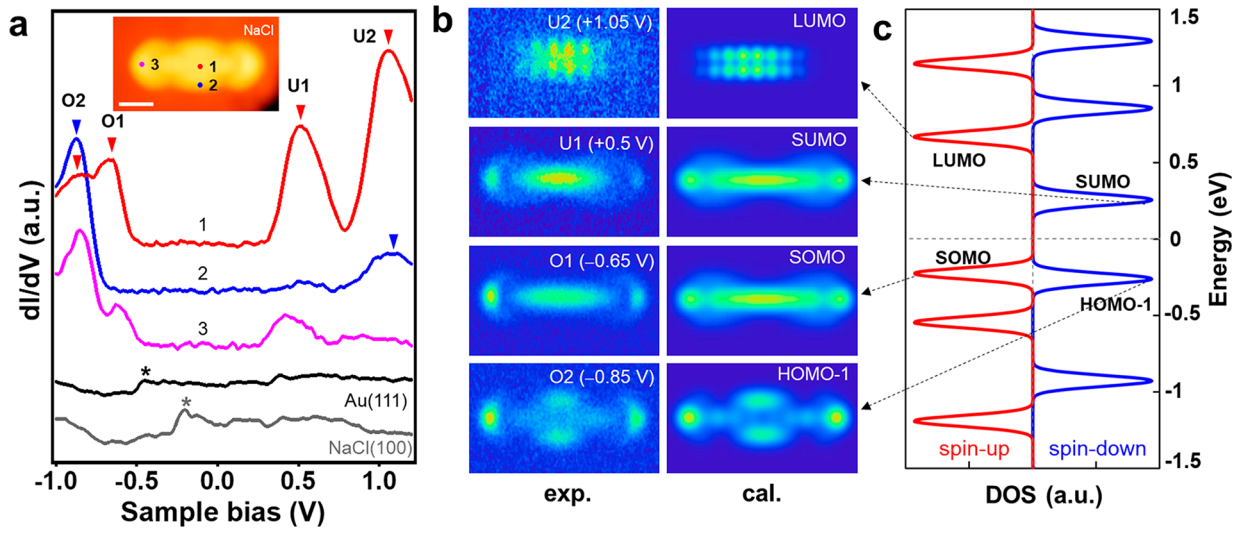

Figure 3. Electronic properties of an LP oligomer on NaCl/Au(111) and the calculated results. (a) dI/dV spectra recorded on different locations (marked in the inset STM image) of the oligomer. The black and gray curves were taken on a bare Au(111) surface and NaCl/Au(111), demonstrating the Shockley surface state of Au(111) at around −0.4 V and the interface state of NaCl/Au(111) at −0.2 V, respectively. Inset: STM topographic image of the oligomer on NaCl/Au(111) (U = −1.0 V, I = 10 pA). Scale bar: 1 nm. (b) Left column: constant-height dI/dV maps conducted at energies of the U2, U1, O1, and O2 states indicated in (a). Right column: calculated LDOS of LUMO, SUMO, SOMO, and HOMO−1 of the oligomer. (c) Spin-resolved density of states for the singly positively charged oligomer. The Fermi level is set to zero.

that no observed coupling products were produced at 433 K, and only a few short chains with terminals having branched chains (indicated by the black-dotted frame in Figure S5c and d) were absorbed along the edge of the terrace on the Au(111) surfaces treated at 473 and 513 K (Figure S5c and d, respectively). These results demonstrate that the methyl groups not only control the selectivity of the [2+2] cycloaddition via methyl-derived steric hindrance but also increase the reactivity of the debrominative [2+2] cycloaddition of TBDB, possibly because of the electron-donating effect of the methyl groups.

Differential conductance spectroscopy (dI/dV) was performed to characterize the electronic structure of the Me-modified LPs. The electronic states of the substrate are dominant in the dI/dV spectra of the LP chain adsorbed on Au(111) (Figure S6), thus preventing the identification of the electronic states of individual chains. Therefore, we dragged an LP oligomer onto the NaCl island via tip manipulation[64−66] to electrically decouple it from the metallic substrate (Figure S7). The nc-AFM measurement (Figure S8) verifies that the oligomers are intact after the manipulation. A comparison between the experimental and the simulated STM images of the end (Figure S9) suggests that the termini of LPs are passivated by hydrogen atoms.[63]

Figure 3a shows the dI/dV spectra obtained on an LP oligomer with nine benzene rings on NaCl(2 ML)/Au(111). Four resonance states are identified at −0.85 V (O2), −0.65 V (O1), +0.5 V (U1), and +1.05 V (U2) on the backbone region, while the O1 and U1 states are not observed on the edge. The dI/dV spectra acquired along/perpendicular to the chain are shown in Figure S10. To avoid the topographic effect of the bulky methyl groups at the chain edge on dI/dV maps, we performed the dI/dV mapping in the constant-height mode, which facilitates a rational comparison to the calculated local density of states (LDOS). We find that the dI/dV maps (Figure 3b) at O1 and U1 both resemble the LDOS of the highest occupied molecular orbital (HOMO) (Figure S11). The observations are in agreement with the earlier works on molecules adsorbed on electronically decoupling layers,[67−69] where charge transfer results in charged molecules, thus singly occupied (SOMO) or the associated unoccupied (SUMO) molecular orbitals are responsible for the resonance peaks observed in the vicinity of the Fermi level.

We suggest that the LPs oligomer on NaCl is positively charged,[70,71] and calculated its spin-resolved density of states, as shown in Figure 3c. The HOMO of the neutral LPs (Figure S11) splits into a singly occupied and a singly unoccupied state that locate below and above the Fermi energy, respectively. Thus, the two states (O1 and U1) could be assigned as the SOMO and SUMO, and both have the shape of the HOMO. The O2 and U2 states as shown in Figure 3a can also be assigned to HOMO−1 and the lowest unoccupied molecular orbital (LUMO) states, as their experimental dI/dV maps agree well with the calculated results (Figure 3b).

The energy gap between the SOMO and SUMO is measured to be 1.15 eV, much larger than the calculated gap of 0.48 eV (Figure 3c). The underestimation of the energy gap could be understood by the incorrect asymptotic behavior of the Heyd−Scuseria−Ernzerhof (HSE) potential. Further considering the electron affinity (EA) and ionization potential (IP) in our calculation,[68] the corrected SOMO−SUMO gap of a positively charged oligomer is 1.11 eV. The measured gap decreases with the increasing length of oligomers on NaCl (Figure S12), suggesting a reduced Coulomb repulsion energy for longer oligomers resulting from the quantum confinement in the axial direction.[67]

The electronic and magnetic properties of LP chains with infinite length are examined theoretically (Figures S13−S17, Table S1). The band structure and total density of states of Me-modified LPs from DFT calculations reveal an indirect bandgap of 1.25 eV (HSE06 result, SI). The Me-modified LPs and LPs without the methyl groups both show an antiferromagnetic ground state, and their nonmagnetism−antiferromagnetism energy difference is comparable to that of the narrowest zigzag graphene nanoribbon. For an LP oligomer adsorbed on the substrate, its magnetization is affected by

https://doi.org/10.1021/jacs.1c05586
J. Am. Chem. Soc. 2021, 143, 12955−12960

multiple aspects, such as adsorption configurations, charge transfer, and substrate screening effects (Figure S18, Table S2). We carried out dI/dV spectra on the LP oligomers adsorbed on Au(111) and NaCl/Au(111), and no obvious spin excitation or Kondo effect signal has been seen (Figure S19).

In summary, we have demonstrated the atomically precise synthesis of LP chains with more than 50 units on the Au(111) surface via dehalogenative [2+2] cycloaddition. The sterically hindered precursor ensures chemoselectivity and orientational order in the product. The structure and electronic properties of the LPs have been determined using a combination of STM and nc-AFM. STS measurements revealed that the LPs on NaCl are charged, whose SOMO and SUMO are identified by dI/dV maps and corroborated by the DFT calculations.

■ ASSOCIATED CONTENT

Supporting Information

The Supporting Information is available free of charge at https://pubs.acs.org/doi/10.1021/jacs.1c05586.

Detailed descriptions of experimental and theoretical procedures and additional STM and DFT calculation results (PDF)

■ AUTHOR INFORMATION

Corresponding Authors

Mengxi Liu − *CAS Key Laboratory of Standardization and Measurement for Nanotechnology, CAS Center for Excellence in Nanoscience, National Center for Nanoscience and Technology, Beijing 100190, China; University of Chinese Academy of Sciences, Beijing 100049, China;* orcid.org/0000-0001-7009-5269; Email: liumx@nanoctr.cn

Xing-Qiang Shi − *College of Physics Science and Technology, Hebei University, Baoding 071002, China;* orcid.org/0000-0003-2029-1506; Email: shixq20hbu@hbu.edu.cn

Xiaohui Qiu − *CAS Key Laboratory of Standardization and Measurement for Nanotechnology, CAS Center for Excellence in Nanoscience, National Center for Nanoscience and Technology, Beijing 100190, China; University of Chinese Academy of Sciences, Beijing 100049, China*; Email: xhqiu@nanoctr.cn

Pei-Nian Liu − *Key Laboratory for Advanced Materials and Feringa Nobel Prize Scientist Joint Research Center, Frontiers Science Center for Materiobiology and Dynamic Chemistry, School of Chemistry and Molecular Engineering, East China University of Science & Technology, Shanghai 200237, China;* orcid.org/0000-0003-2014-2244; Email: liupn@ecust.edu.cn

Authors

Deng-Yuan Li − *Key Laboratory for Advanced Materials and Feringa Nobel Prize Scientist Joint Research Center, Frontiers Science Center for Materiobiology and Dynamic Chemistry, School of Chemistry and Molecular Engineering, East China University of Science & Technology, Shanghai 200237, China*

Xia Qiu − *CAS Key Laboratory of Standardization and Measurement for Nanotechnology, CAS Center for Excellence in Nanoscience, National Center for Nanoscience and Technology, Beijing 100190, China; University of Chinese Academy of Sciences, Beijing 100049, China; Academy for Advanced Interdisciplinary Studies, Peking University, Beijing 100871, China*

Shi-Wen Li − *Key Laboratory for Advanced Materials and Feringa Nobel Prize Scientist Joint Research Center, Frontiers Science Center for Materiobiology and Dynamic Chemistry, School of Chemistry and Molecular Engineering, East China University of Science & Technology, Shanghai 200237, China*

Yin-Ti Ren − *College of Physics Science and Technology, Hebei University, Baoding 071002, China*

Ya-Cheng Zhu − *Key Laboratory for Advanced Materials and Feringa Nobel Prize Scientist Joint Research Center, Frontiers Science Center for Materiobiology and Dynamic Chemistry, School of Chemistry and Molecular Engineering, East China University of Science & Technology, Shanghai 200237, China*

Chen-Hui Shu − *Key Laboratory for Advanced Materials and Feringa Nobel Prize Scientist Joint Research Center, Frontiers Science Center for Materiobiology and Dynamic Chemistry, School of Chemistry and Molecular Engineering, East China University of Science & Technology, Shanghai 200237, China*

Xiao-Yu Hou − *CAS Key Laboratory of Standardization and Measurement for Nanotechnology, CAS Center for Excellence in Nanoscience, National Center for Nanoscience and Technology, Beijing 100190, China; University of Chinese Academy of Sciences, Beijing 100049, China*

Complete contact information is available at: https://pubs.acs.org/10.1021/jacs.1c05586

Author Contributions

#D.-Y.L., X.Q., S.-W.L., and Y.-T.R. contributed equally to this work.

Notes

The authors declare no competing financial interest.

■ ACKNOWLEDGMENTS

This work was supported by the National Natural Science Foundation of China (21925201, 91845110, 21972032, 21790353, 21721002, 21425310, and 21978049), Shanghai Municipal Science and Technology Major Project (2018SHZDZX03), Natural Science Foundation of Shanghai (20ZR1414200), the Programme of Introducing Talents of Discipline to Universities (B16017), the Ministry of Science and Technology of China (2017YFA0205000), the Strategic Priority Research Program of Chinese Academy of Sciences (XDB36000000), the Scientific Instrument Developing Project of the Chinese Academy of Sciences (GJJSTD20200005), Advanced Talents Incubation Program of Hebei University (521000981390), and the Program for Eastern Scholar Distinguished Professor. We thank the High-performance Computing Center of Hebei University and the Research Center of Analysis and Test of East China University of Science and Technology for help in the characterization.

■ REFERENCES

(1) Yu, L.; Chen, M.; Dalton, L. R. Ladder Polymers: Recent Developments in Syntheses, Characterization, and Potential Applications as Electronic and Optical Materials. *Chem. Mater.* **1990**, *2*, 649−659.

(2) Scherf, U. Ladder-type materials. *J. Mater. Chem.* **1999**, *9*, 1853−1864.

(3) Sakamoto, J.; van Heijst, J.; Lukin, O.; Schluter, A. D. Two-dimensional polymers: just a dream of synthetic chemists? *Angew. Chem., Int. Ed.* **2009**, *48*, 1030−1069.

(4) Lee, J.; Kalin, A. J.; Yuan, T.; Al-Hashimi, M.; Fang, L. Fully conjugated ladder polymers. *Chem. Sci.* **2017**, *8*, 2503−2521.
(5) Cai, Z.; Awais, M. A.; Zhang, N.; Yu, L. Exploration of Syntheses and Functions of Higher Ladder-type π-Conjugated Heteroacenes. *Chem.* **2018**, *4*, 2538−2570.
(6) Zhu, C.; Fang, L. Locking the Coplanar Conformation of π-Conjugated Molecules and Macromolecules Using Dynamic Noncovalent Bonds. *Macromol. Rapid Commun.* **2018**, *39*, 1700241.
(7) Zhu, C.; Kalin, A. J.; Fang, L. Covalent and Noncovalent Approaches to Rigid Coplanar pi-Conjugated Molecules and Macromolecules. *Acc. Chem. Res.* **2019**, *52*, 1089−1100.
(8) Prins, P.; Grozema, F. C.; Schins, J. M.; Patil, S.; Scherf, U.; Siebbeles, L. D. A. High Intrachain Hole Mobility on Molecular Wires of Ladder-Type Poly(*p*-Phenylenes). *Phys. Rev. Lett.* **2006**, *96*, 146601.
(9) Babel, A.; Jenekhe, S. A. High Electron Mobility in Ladder Polymer Field-Effect Transistors. *J. Am. Chem. Soc.* **2003**, *125*, 13656−13657.
(10) Samiullah, M.; Moghe, D.; Scherf, U.; Guha, S. Diffusion length of triplet excitons in organic semiconductors. *Phys. Rev. B: Condens. Matter Mater. Phys.* **2010**, *82*, 205211.
(11) Tsuda, A.; Osuka, A. Fully Conjugated Porphyrin Tapes with Electronic Absorption Bands That Reach into Infrared. *Science* **2001**, *293*, 79−82.
(12) Yang, W.; Lucotti, A.; Tommasini, M.; Chalifoux, W. A. Bottom-Up Synthesis of Soluble and Narrow Graphene Nanoribbons Using Alkyne Benzannulations. *J. Am. Chem. Soc.* **2016**, *138*, 9137−9144.
(13) Toda, F.; Garratt, P. Four-Membered Ring Compounds Containing Bis(Methylene)Cyclobutene or Tetrakis(Methylene)-Cyclobutane Moieties. Benzocyclobutadiene, Benzodicyclobutadiene, Biphenylene, and Related Compounds. *Chem. Rev.* **1992**, *92*, 1685−1707.
(14) Vollhardt, K. P. C. The phenylenes. *Pure Appl. Chem.* **1993**, *65*, 153−156.
(15) Baumgarten, M.; Dietz, F.; Müllen, K.; Karabunarliev, S.; Tyutyulkov, N. Energy spectra of infinite phenylenes. *Chem. Phys. Lett.* **1994**, *221*, 71−74.
(16) Rajca, A.; Safronov, A.; Rajica, S.; Ross, C. R., II; Stezowski, J. J. Biphenylene Dimer. Molecular Fragment of a Two-Dimensional Carbon Net and Double-Stranded Polymer. *J. Am. Chem. Soc.* **1996**, *118*, 7272−7279.
(17) Albright, T. A.; Dosa, P. I.; Grossmann, T. N.; Khrustalev, V. N.; Oloba, O. A.; Padilla, R.; Paubelle, R.; Stanger, A.; Timofeeva, T. V.; Vollhardt, K. P. C. Photo-Thermal Haptotropism in Cyclopentadienylcobalt Complexes of Linear Phenylenes: Intercyclobutadiene Metal Migration. *Angew. Chem., Int. Ed.* **2009**, *48*, 9853−9857.
(18) Albright, T. A.; Oldenhof, S.; Oloba, O. A.; Padilla, R.; Vollhardt, K. P. C. Reversible intercyclobutadiene haptotropism in cyclopentadienylcobalt linear [4]phenylene. *Chem. Commun.* **2011**, *47*, 9039−9041.
(19) Schulman, J. M.; Disch, R. L. Theroretical Studies of the [*N*]Phenylenes. *J. Am. Chem. Soc.* **1996**, *118*, 8470−8474.
(20) Manzetti, S.; Lu, T. Alternant conjugated oligomers with tunable and narrow HOMO−LUMO gaps as sustainable nanowires. *RSC Adv.* **2013**, *3*, 25881−25890.
(21) Cui, P.; Zhang, Q.; Zhu, H.; Li, X.; Wang, W.; Li, Q.; Zeng, C.; Zhang, Z. Carbon Tetragons as Definitive Spin Switches in Narrow Zigzag Graphene Nanoribbons. *Phys. Rev. Lett.* **2016**, *116*, 026802.
(22) Lothrop, W. C. Biphenylene. *J. Am. Chem. Soc.* **1941**, *63*, 1187−1191.
(23) Berris, B. C.; Hovakeemian, G. H.; Lai, Y.-H.; Mestdagh, H.; Vollhardt, K. P. C. A new approach to the construction of biphenylenes by the cobalt-catalyzed cocyclization of *o*-diethynylbenzenes with alkynes. Application to an iterative approach to [3]phenylene, the first member of a novel class of benzocyclobutadienoid hydrocarbons. *J. Am. Chem. Soc.* **1985**, *107*, 5670−5687.
(24) Hirthammer, M.; Vollhardt, K. P. C. 2,3-Bis(trimethylsilyl)- and 2,3,8,9-Tetrakis(trimethylsilyl)[4]phenylene. *J. Am. Chem. Soc.* **1986**, *108*, 2482−2484.
(25) Blanco, L.; Helson, H. E.; Hirthammer, M.; Mestdagh, H.; Spyroudis, S.; Vollhardt, K. P. C. 2,3,9,10-Tetrakis(trimethylsilyl)[5]-phenylene. Synthesis via Regiospecific Cobalt-Catalyzed Cocyclization of 1,6-Bis(triisopropylsilyl)-1,3,5-hexatriyne. *Angew. Chem., Int. Ed. Engl.* **1987**, *26*, 1246−1247.
(26) Dosche, C.; Löhmannsröben, H.-G.; Bieser, A.; Dosa, P. I.; Han, S.; Iwamoto, M.; Schleifenbaum, A.; Vollhardt, K. P. C. Photophysical properties of [*N*]phenylenes. *Phys. Chem. Chem. Phys.* **2002**, *4*, 2156−2161.
(27) Dosche, C.; Kumke, M. U.; Ariese, F.; Bader, A. N.; Gooijer, C.; Dosa, P. I.; Han, S.; Miljanić, O. Š.; Vollhardt, K. P. C.; Puchta, R.; van Eikema Hommes, N. J. R. Shpol'skii spectroscopy and vibrational analysis of [*N*]phenylenes. *Phys. Chem. Chem. Phys.* **2003**, *5*, 4563−4569.
(28) Dosche, C.; Kumke, M. U.; Löhmannsröben, H. G.; Ariese, F.; Bader, A. N.; Gooijer, C.; Miljanić, O. Š.; Iwamoto, M.; Vollhardt, K. P. C.; Puchta, R.; van Eikema Hommes, N. J. R. Deuteration effects on the vibronic structure of the fluorescence spectra and the internal conversion rates of triangular [4]phenylene. *Phys. Chem. Chem. Phys.* **2004**, *6*, 5476−5483.
(29) Dosche, C.; Mickler, W.; Löhmannsröben, H.-G.; Agenet, N.; Vollhardt, K. P. C. Photoinduced electron transfer in [*N*]phenylenes. *J. Photochem. Photobiol., A* **2007**, *188*, 371−377.
(30) Clair, S.; de Oteyza, D. G. Controlling a Chemical Coupling Reaction on a Surface: Tools and Strategies for On-Surface Synthesis. *Chem. Rev.* **2019**, *119*, 4717−4776.
(31) Klappenberger, F.; Zhang, Y.-Q.; Björk, J.; Klyatskaya, S.; Ruben, M.; Barth, J. V. On-Surface Synthesis of Carbon-Based Scaffolds and Nanomaterials Using Terminal Alkynes. *Acc. Chem. Res.* **2015**, *48*, 2140−2150.
(32) Mishra, S.; Beyer, D.; Eimre, K.; Liu, J.; Berger, R.; Gröning, O.; Pignedoli, C. A.; Müllen, K.; Fasel, R.; Feng, X.; Ruffieux, P. Synthesis and Characterization of π-Extended Triangulene. *J. Am. Chem. Soc.* **2019**, *141*, 10621−10625.
(33) Su, J.; Telychko, M.; Hu, P.; Macam, G.; Mutombo, P.; Zhang, H.; Bao, Y.; Cheng, F.; Huang, Z.-Q.; Qiu, Z.; Tan, S. J. R.; Lin, H.; Jelínek, P.; Chuang, F.-C.; Wu, J.; Lu, J. Atomically precise bottom-up synthesis of π-extended [5]triangulene. *Sci. Adv.* **2019**, *5*, No. eaav7717.
(34) Li, D.-Y.; Li, S.-W.; Xie, Y.-L.; Hua, X.; Long, Y.-T.; Wang, A.; Liu, P.-N. On-surface synthesis of planar dendrimers via divergent cross-coupling reaction. *Nat. Commun.* **2019**, *10*, 2414.
(35) Fan, Q.; Martin-Jimenez, D.; Werner, S.; Ebeling, D.; Koehler, T.; Vollgraff, T.; Sundermeyer, J.; Hieringer, W.; Schirmeisen, A.; Gottfried, J. M. On-Surface Synthesis and Characterization of a Cycloarene: C108 Graphene Ring. *J. Am. Chem. Soc.* **2020**, *142*, 894−899.
(36) Mishra, S.; Beyer, D.; Eimre, K.; Kezilebieke, S.; Berger, R.; Gröning, O.; Pignedoli, C. A.; Müllen, K.; Liljeroth, P.; Ruffieux, P.; Feng, X.; Fasel, R. Topological frustration induces unconventional magnetism in a nanographene. *Nat. Nanotechnol.* **2020**, *15*, 22−28.
(37) Mishra, S.; Yao, X.; Chen, Q.; Eimre, K.; Gröning, O.; Ortiz, R.; Di Giovannantonio, M.; Sancho-García, J. C.; Fernández-Rossier, J.; Pignedoli, C. A.; Müllen, K.; Ruffieux, P.; Narita, A.; Fasel, R. Large Magnetic Exchange Coupling in Rhombus-Shaped Nanographenes with Zigzag Periphery. *Nat. Chem.* **2021**, *13*, 581−586.
(38) Grill, L.; Hecht, S. Covalent on-surface polymerization. *Nat. Chem.* **2020**, *12*, 115−130.
(39) Shu, C.-H.; Liu, M.-X.; Zha, Z.-Q.; Pan, J.-L.; Zhang, S.-Z.; Xie, Y.-L.; Chen, J.-L.; Yuan, D.-W.; Qiu, X.-H.; Liu, P.-N. On-surface synthesis of poly(*p*-phenylene ethynylene) molecular wires via in situ formation of carbon-carbon triple bond. *Nat. Commun.* **2018**, *9*, 2322.
(40) Sánchez-Sánchez, C.; Dienel, T.; Nicolaï, A.; Kharche, N.; Liang, L.; Daniels, C.; Meunier, V.; Liu, J.; Feng, X.; Müllen, K.; Sánchez-Valencia, J. R.; Gröning, O.; Ruffieux, P.; Fasel, R. On-Surface Synthesis and Characterization of Acene-Based Nanoribbons

https://doi.org/10.1021/jacs.1c05586
J. Am. Chem. Soc. 2021, 143, 12955−12960

Incorporating Four-Membered Rings. *Chem. - Eur. J.* **2019**, *25*, 12074−12082.
(41) de la Torre, B.; Matěj, A.; Sánchez-Grande, A.; Cirera, B.; Mallada, B.; Rodríguez-Sánchez, E.; Santos, J.; Mendieta-Moreno, J. I.; Edalatmanesh, S.; Lauwaet, K.; Otyepka, M.; Medved', M.; Buendía, Á.; Miranda, R.; Martín, N.; Jelínek, P.; Écija, D. Tailoring π-conjugation and vibrational modes to steer on-surface synthesis of pentalene-bridged ladder polymers. *Nat. Commun.* **2020**, *11*, 4567.
(42) Cirera, B.; Sánchez-Grande, A.; de la Torre, B.; Santos, J.; Edalatmanesh, S.; Rodríguez-Sánchez, E.; Lauwaet, K.; Mallada, B.; Zbořil, R.; Miranda, R.; Gröning, O.; Jelínek, P.; Martín, N.; Ecija, D. Tailoring topological order and π-conjugation to engineer quasi-metallic polymers. *Nat. Nanotechnol.* **2020**, *15*, 437−443.
(43) Talirz, L.; Ruffieux, P.; Fasel, R. On-Surface Synthesis of Atomically Precise Graphene Nanoribbons. *Adv. Mater.* **2016**, *28*, 6222−6231.
(44) Cai, J.; Ruffieux, P.; Jaafar, R.; Bieri, M.; Braun, T.; Blankenburg, S.; Muoth, M.; Seitsonen, A. P.; Saleh, M.; Feng, X.; Müllen, K.; Fasel, R. Atomically precise bottom-up fabrication of graphene nanoribbons. *Nature* **2010**, *466*, 470−473.
(45) Ruffieux, P.; Wang, S.; Yang, B.; Sánchez-Sánchez, C.; Liu, J.; Dienel, T.; Talirz, L.; Shinde, P.; Pignedoli, C. A.; Passerone, D.; Dumslaff, T.; Feng, X.; Müllen, K.; Fasel, R. On-surface synthesis of graphene nanoribbons with zigzag edge topology. *Nature* **2016**, *531*, 489−492.
(46) Gröning, O.; Wang, S.; Yao, X.; Pignedoli, C. A.; Borin Barin, G.; Daniels, C.; Cupo, A.; Meunier, V.; Feng, X.; Narita, A.; Müllen, K.; Ruffieux, P.; Fasel, R. Engineering of robust topological quantum phases in graphene nanoribbons. *Nature* **2018**, *560*, 209−213.
(47) Rizzo, D. J.; Veber, G.; Cao, T.; Bronner, C.; Chen, T.; Zhao, F.; Rodriguez, H.; Louie, S. G.; Crommie, M. F.; Fischer, F. R. Topological band engineering of graphene nanoribbons. *Nature* **2018**, *560*, 204−208.
(48) Liu, M.; Liu, M.; She, L.; Zha, Z.; Pan, J.; Li, S.; Li, T.; He, Y.; Cai, Z.; Wang, J.; Zheng, Y.; Qiu, X.; Zhong, D. Graphene-like nanoribbons periodically embedded with four- and eight-membered rings. *Nat. Commun.* **2017**, *8*, 14924.
(49) Grill, L.; Dyer, M.; Lafferentz, L.; Persson, M.; Peters, M. V.; Hecht, S. Nano-architectures by covalent assembly of molecular building blocks. *Nat. Nanotechnol.* **2007**, *2*, 687−691.
(50) Moreno, C.; Vilas-Varela, M.; Kretz, B.; Garcia-Lekue, A.; Costache, M. V.; Paradinas, M.; Panighel, M.; Ceballos, G.; Valenzuela, S. O.; Peña, D.; Mugarza, A. Bottom-up Synthesis of Multifunctional Nanoporous Graphene. *Science* **2018**, *360*, 199−203.
(51) Jacobse, P. H.; McCurdy, R. D.; Jiang, J.; Rizzo, D. J.; Veber, G.; Butler, P.; Zuzak, R.; Louie, S. G.; Fischer, F. R.; Crommie, M. F. Bottom-up Assembly of Nanoporous Graphene with Emergent Electronic States. *J. Am. Chem. Soc.* **2020**, *142*, 13507−13514.
(52) Galeotti, G.; De Marchi, F.; Hamzehpoor, E.; MacLean, O.; Rajeswara Rao, M.; Chen, Y.; Besteiro, L. V.; Dettmann, D.; Ferrari, L.; Frezza, F.; Sheverdyaeva, P. M.; Liu, R.; Kundu, A. K.; Moras, P.; Ebrahimi, M.; Gallagher, M. C.; Rosei, F.; Perepichka, D. F.; Contini, G. Synthesis of mesoscale ordered two-dimensional pi-conjugated polymers with semiconducting properties. *Nat. Mater.* **2020**, *19*, 874−880.
(53) Fan, Q.; Yan, L.; Tripp, M. W.; Chen, M.; Foster, A. S.; Koert, U.; Liljeroth, P.; Gottfried, J. M. Biphenylene Sheet: A Nonbenzenoid Carbon Allotrope. *Science* **2021**, *372*, 852−856.
(54) Bian, K.; Gerber, C.; Heinrich, A. J.; Müller, D. J.; Scheuring, S.; Jiang, Y. Scanning probe microscopy. *Nat. Rev. Meth. Primers* **2021**, *1*, 36.
(55) Sánchez-Sánchez, C.; Nicolai, A.; Rossel, F.; Cai, J.; Liu, J.; Feng, X.; Müllen, K.; Ruffieux, P.; Fasel, R.; Meunier, V. On-Surface Cyclization of ortho-Dihalotetracenes to Four- and Six-Membered Rings. *J. Am. Chem. Soc.* **2017**, *139*, 17617−17623.
(56) Zhang, C.; Kazuma, E.; Kim, Y. Atomic-Scale Visualization of the Stepwise Metal-Mediated Dehalogenative Cycloaddition Reaction Pathways: Competition between Radicals and Organometallic Intermediates. *Angew. Chem., Int. Ed.* **2019**, *58*, 17736−17744.
(57) Zhang, R.; Xia, B.; Xu, H.; Lin, N. Identifying Multinuclear Organometallic Intermediates in On-Surface [2 + 2] Cycloaddition Reactions. *Angew. Chem., Int. Ed.* **2019**, *58*, 16485−16489.
(58) Gao, H. Y.; Wagner, H.; Zhong, D.; Franke, J. H.; Studer, A.; Fuchs, H. Glaser coupling at metal surfaces. *Angew. Chem., Int. Ed.* **2013**, *52*, 4024−4028.
(59) Liu, J.; Xia, B.; Xu, H.; Lin, N. Controlling the Reaction Steps of Bifunctional Molecules 1,5-Dibromo-2,6-dimethylnaphthalene on Different Substrates. *J. Phys. Chem. C* **2018**, *122*, 13001−13008.
(60) Fritton, M.; Otte, K.; Bjork, J.; Biswas, P. K.; Heckl, W. M.; Schmittel, M.; Lackinger, M. The influence of ortho-methyl substitution in organometallic self-assembly - a comparative study on Cu(111) vs. Ag(111). *Chem. Commun.* **2018**, *54*, 9745−9748.
(61) Fan, Q.; Werner, S.; Tschakert, J.; Ebeling, D.; Schirmeisen, A.; Hilt, G.; Hieringer, W.; Gottfried, J. M. Precise Monoselective Aromatic C-H Bond Activation by Chemisorption of Meta-Aryne on a Metal Surface. *J. Am. Chem. Soc.* **2018**, *140*, 7526−7532.
(62) Telychko, M.; Su, J.; Gallardo, A.; Gu, Y.; Mendieta-Moreno, J. I.; Qi, D.; Tadich, A.; Song, S.; Lyu, P.; Qiu, Z.; Fang, H.; Koh, M. J.; Wu, J.; Jelinek, P.; Lu, J. Strain-Induced Isomerization in One-Dimensional Metal-Organic Chains. *Angew. Chem., Int. Ed.* **2019**, *58*, 18591−18597.
(63) Pavliček, N.; Schuler, B.; Collazos, S.; Moll, N.; Pérez, D.; Guitián, E.; Meyer, G.; Peña, D.; Gross, L. On-surface generation and imaging of arynes by atomic force microscopy. *Nat. Chem.* **2015**, *7*, 623−628.
(64) Wang, S.; Talirz, L.; Pignedoli, C. A.; Feng, X.; Müllen, K.; Fasel, R.; Ruffieux, P. Giant edge state splitting at atomically precise graphene zigzag edges. *Nat. Commun.* **2016**, *7*, 11507.
(65) Lawrence, J.; Brandimarte, P.; Berdonces-Layunta, A.; Mohammed, M. S. G.; Grewal, A.; Leon, C. C.; Sánchez-Portal, D.; de Oteyza, D. G. Probing the Magnetism of Topological End States in 5-Armchair Graphene Nanoribbons. *ACS Nano* **2020**, *14*, 4499−4508.
(66) Jacobse, P. H.; Mangnus, M. J. J.; Zevenhuizen, S. J. M.; Swart, I. Mapping the Conductance of Electronically Decoupled Graphene Nanoribbons. *ACS Nano* **2018**, *12*, 7048−7056.
(67) Cochrane, K. A.; Schiffrin, A.; Roussy, T. S.; Capsoni, M.; Burke, S. A. Pronounced Polarization-Induced Energy Level Shifts at Boundaries of Organic Semiconductor Nanostructures. *Nat. Commun.* **2015**, *6*, 8312.
(68) Hollerer, M.; Lüftner, D.; Hurdax, P.; Ules, T.; Soubatch, S.; Tautz, F. S.; Koller, G.; Puschnig, P.; Sterrer, M.; Ramsey, M. G. Charge Transfer and Orbital Level Alignment at Inorganic/Organic Interfaces: The Role of Dielectric Interlayers. *ACS Nano* **2017**, *11*, 6252−6260.
(69) Kimura, K.; Miwa, K.; Imada, H.; Imai-Imada, M.; Kawahara, S.; Takeya, J.; Kawai, M.; Galperin, M.; Kim, Y. Selective Triplet Exciton Formation in a Single Molecule. *Nature* **2019**, *570*, 210−213.
(70) The ionization potential of the LP oligomer is calculated to be 3.3 eV, which is lower than the work function of NaCl/Au(111) (4.3 eV),[71] suggesting that the LP oligomers could be positively charged on NaCl/Au(111).
(71) Li, Z.; Chen, H.-Y. T.; Schouteden, K.; Janssens, E.; Van Haesendonck, C.; Lievens, P.; Pacchioni, G. Spontaneous Doping of Two-Dimensional NaCl Films with Cr Atoms: Aggregation and Electronic Structure. *Nanoscale* **2015**, *7*, 2366−2373.

https://doi.org/10.1021/jacs.1c05586
J. Am. Chem. Soc. 2021, 143, 12955−12960